Chimeric 3D-gastruloids – a versatile tool for studies of mammalian peri-gastrulation development

Alexandra E. Wehmeyer[1], Katrin M. Schüle[1], Alexandra Conrad[1], Chiara M. Schröder[1,2,3,4], Simone Probst[1], and Sebastian J. Arnold[1,4]

[1]Institute of Experimental and Clinical Pharmacology and Toxicology, Faculty of Medicine, University of Freiburg, Albertstrasse 25, D-79104 Freiburg, Germany
[2]Spemann Graduate School of Biology and Medicine (SGBM), University of Freiburg, Albertstrasse 19a, D-79104 Freiburg, Germany
[3]Faculty of Biology, University of Freiburg, Schänzlestrasse 1, D-79104 Freiburg, Germany
[4]Signaling Research Centers BIOSS and CIBSS, University of Freiburg, Schänzlestrasse18, D-79104 Freiburg, Germany

Correspondence should be addressed to sebastian.arnold@pharmakol.uni-freiburg.de

ORCID Alexandra E. Wehmeyer 0000-0002-9981-8042
ORCID Katrin M. Schüle 0000-0001-6642-0030
ORCID Alexandra Conrad 0000-0001-7766-5033
ORCID Chiara M. Schröder 0000-0001-5345-3415
ORCID Simone Probst 0000-0002-0220-5400
ORCID Sebastian J. Arnold 0000-0002-2688-9210

Key words

Chimeric *3D*-Gastruloids, mESCs, functional genetics, Tbx transcription factors, *Eomes*, *Brachyury*

Abstract

Stem cell-derived 3D-gastruloids show a remarkable capacity of self-organisation and recapitulate many aspects of gastrulation stage mammalian development. Gastruloids can be rapidly generated and offer several experimental advantages, such as scalability, observability, and accessibility for experimental manipulation. Here, we present innovative approaches to further expand the experimental potency of 3D-gastruloids by combining it with functional genetics in embryonic stem cells (ESCs) and the generation of chimeric gastruloids. Chimeric gastruloids are composed of fluorescently labelled cells of different genotypes for example cells with inducible gene-expression, or loss-of-gene function, combined with wildtype cells. We showcase the experimental approach and some advantages of chimeric gastruloids using ESCs carrying homozygous deletions of the Tbx transcription factors *Brachyury* or inducible expression of *Eomes.* The resulting chimeric gastruloids allowed to discriminate cell-autonomous from non-autonomous gene functions that normally are difficult to observe by genetics in the embryo.

Introduction

The versatile experimental opportunities offered by functional genetics available in the mouse as main mammalian model system have greatly enhanced our understanding of embryonic development. However, studies of mammalian embryogenesis are hampered by the relative inaccessibility of the embryo due to intrauterine growth. *Ex vivo* embryo cultures partially overcome some of the experimental restrictions but rely on the isolation of often limiting numbers of embryos. More recently, novel approaches were developed to generate stem cell derived, 3D-embryoids reflecting different stages of mammalian development from the formation of the blastocyst (Kagawa et al., 2022; Li et al., 2019; Yu et al., 2021), to periimplantation embryos (Amadei et al., 2021; Harrison et al., 2017; Harrison et al., 2018), and postimplantation stages recapitulating early organogenesis (Beccari et al., 2018; Moris et al., 2020; Turner et al., 2017; van den Brink et al., 2020; van den Brink et al., 2014; Veenvliet et al., 2020). These embryoid models demonstrate the remarkable self-organisation and robustness of embryonic programs that guide the processes of morphogenesis, growth, cell lineage specification and differentiation.

Among the most widely used embryoid model system are 3D-gastruloids, offering a simple experimental procedure to reproducibly generate embryoids that recapitulate development stages from early gastrulation to somitogenesis and onset of

organogenesis (comparable to Embryonic days 6.5 (E6.5) – E9.0) reviewed in (van den Brink and van Oudenaarden, 2021; Veenvliet et al., 2021). 3D-gastruloids are formed by the aggregation of 100-300 mouse or human pluripotent embryonic stem cells (ESCs) that are treated by a 24 h pulse of the GSK3β-inhibitor CHIR to activate the canonical Wnt-cascade. This signalling stimulus induces an anterior-posterior asymmetry in the aggregate (van den Brink et al., 2014), indicated by the one-sided expression of the Tbx factor *Brachyury* that in the embryo marks the site of primitive streak formation at gastrulation onset (Rivera-Perez and Magnuson, 2005; reviewed in Arnold and Robertson, 2009). The *Brachyury*-expressing posterior pole of 3D-gastruloids elongates over several days thereby forming different tissues resembling paraxial mesoderm, neural tube, and the primitive gut tube. 3D-gastruloids show a remarkable self-organizing capacity as the different tissues are generated in proper spatial organization and arranged according to the embryonic axes (Beccari et al., 2018). 3D-gastruloids thus can be used as model systems for studies of various gastrulation-associated morphogenetic processes, as exemplified for somitogenesis (van den Brink et al., 2020; Veenvliet et al., 2020). However, some tissues of gastrulation stage embryos are less represented in 3D-organoids, including anterior mesoderm derivatives, such as cardiogenic mesoderm, and cranial structures such as cranial neural tissues (van den Brink et al., 2020; Veenvliet et al., 2020). This underrepresentation of anterior/cranial tissues most likely results from the initial induction of ESC aggregates with CHIR which imposes a strong signal for posterior/caudal tissue identity (Dunty et al., 2008). However, this and other aberrations of 3D-gastruloids compared to embryos can also be used to investigate which additional regulatory requirements need to be met for proper morphogenesis of tissues and organ *anlagen* to more closely recapitulate the embryo (Veenvliet et al., 2021). Due to the scalability of this ESC- derived embryoid culture system, multiple different environmental cues can be readily tested. It is thus expected that further refinements of current protocols will lead to the generation of gastruloids that more closely resemble the different aspects of embryogenesis.

Cell specification to mesoderm and definitive endoderm (DE) cell lineages is regulated by two Tbx transcription factors *Eomesodermin* (*Eomes*) and *Brachyury (T)*. Functions of both factors were previously extensively studied establishing crucial roles of *Eomes* for cell lineage specification of definitive endoderm (DE) (Arnold et al., 2008; Teo et al., 2011) and anterior mesoderm (Costello et al., 2011), and functions of *Brachyury*

for the generation of posterior mesoderm derivatives, and notochord (Wymeersch et al., 2021). The compound genetic deletion of *Eomes* and *Brachyury* completely abrogates specification of any ME during differentiation of pluripotent cells (Tosic et al., 2019). While functions of these Tbx factors for specification of cell fate are well described, their roles in tissue-wide morphogenetic processes are less obvious. For example, the genetic deletion of *Eomes* in the epiblast abrogates formation of the mesoderm (and DE) cell layer, hindering studies of morphogenetic functions of *Eomes*-regulated programs (Arnold et al., 2008). Similarly, studies of the role of *Brachyury* in posterior body axis extension are compromised by cell non-autonomous functions of *Brachyury* in feed-forward regulatory loops to maintain caudal Wnt-signals, also acting on cell specification and morphogenetic programs (Arnold et al., 2000; Dunty et al., 2008; Martin and Kimelman, 2008; Turner et al., 2014; Yamaguchi et al., 1999).

In this report, we demonstrate an approach to further expand the experimental potency of 3D-gastruloids. We use genetically engineered, traceable ESCs to generate chimeric 3D-gastruloids that are composed of cells with different genotypes. To showcase the advantages of this approach and to test experimental feasibility we generated fluorescently labelled ESC lines with homozygous loss-of-function, or inducible expression cassettes for the two Tbx transcription factors *Eomes* and *Brachyury*. These are used to generate chimeric gastruloids, e.g. by mixing inducible Tbx-expressing, or Tbx-deficient and WT cells to generate complex genetic situations that are normally only difficult to achieve by conventional genetic tools in embryos. In addition to demonstrating the efficiency and feasibility of this experimental approach of chimeric gastruloids, this study also provides insights into some of the morphogenetic function of *Eomes* and *Brachyury*, which could not be achieved using genetic approaches in embryos.

Results and Discussion

To expand the experimental versatility of the 3D-gastruloid model system we combined it with the use of genetically modified ESCs and fluorescent imaging approaches. We generated chimeric gastruloids composed of cells with different genetic backgrounds that can be readily traced by microscopic observation using fluorescent membrane labels (Fig. 1A, B). We generated WT ESCs that are permanently labelled by knock-in of membrane GFP (mG) into the Rosa26 genomic locus (Fig. 1C). Membrane Tomato (mT) labelling was used for genetically manipulated ESCs (Fig. 1C). Genetic

alterations used in presented experiments were the genetic deletion of the Tbx transcription factor *Brachyury* (*Bra*$^{-/-}$), and the ICE-mediated (induced cassette exchange) targeted integration of *Eomes* 3' to a Tet-responsive element (TRE) in A2lox ESCs (Iacovino et al., 2014). We tested the generation of chimeric gastruloids by two approaches (Fig. 1D, E). Either by mixing of different cells during the aggregation of ESCs at the beginning of gastruloid culture (Fig. 1E), or by merging of two preformed ESCs aggregates composed of different cells before CHIR-induction (Fig. 1D). ESC-generated aggregates rapidly fuse and stably adhere after placing them together in 96-wells (Fig. 1D) or in hanging drops (not shown). The mixing of cells at different ratios can be used to evaluate cell-autonomous vs. cell non-autonomous gene functions, by testing how different levels of cell contribution affects tissue-behaviour, e.g. when using cells with loss-of-gene-function. Merging of cell aggregates can be applied when the behaviour of coherent groups of cells is analysed, such as in studies of inductive tissue interactions. A similar approach was recently reported where a small aggregate of 50 cells was treated with BMP4 to induce organizer-activities which was used instead of CHIR-treatment for the induction of gastruloid-formation (Xu et al., 2021). Thus, chimeric gastruloids offer multiple experimental opportunities to study gastrulation development (Fig. 1A) as exemplarily demonstrated in following experiments.

First, we tested if chimeric gastruloids are a suitable model to study instructive gene functions during lineage specification. Hence, we generated chimeric gastruloids by merging preformed aggregates of WT ESCs (mG) and ESCs containing a doxycycline (Dox) inducible GFP-tagged expression cassette for the Tbx factor *EomesGFP* (mT) (Fig. 2A, B). *Eome*s is crucially required for lineage specification towards definitive endoderm (Arnold et al., 2008; Teo et al., 2011) and anterior mesoderm, including the cardiac lineage (Costello et al., 2011; Probst et al., 2021). We tested if forced *Eomes* expression in a group of cells (TRE.*EomesGFP*) within a gastruloid would be sufficient to induce a coherent heart-like domain, which is only inconsistently occurring in gastruloids formed of WT ESCs (Rossi et al., 2021; van den Brink and van Oudenaarden, 2021). Indeed, Dox-induced *EomesGFP*-expressing cells form a domain of beating cardiomyocytes (Fig. 2C, Supplementary movie 2) in chimeric gastruloids in more than 30% of cases, whereas similar beating areas are only very rarely observed in uninduced chimeric gastruloids (Fig. 2D) or using only A2lox WT ESCs (not shown). To correlate induced *EomesGFP* expression with the cardiogenic domain we performed *in situ* hybridization analyses for early cardiac markers *Mlc2a*

and *Nkx2.5*, which are found almost exclusively in mT-marked TRE.*EomesGFP* cells that are forming a coherent domain on one side of gastruloids (Fig. 2E). This experiment thus shows that induced expression of *Eomes* suffices to cell-autonomously generate coherent cardiogenic domains oriented to one side of the developing gastruloid, resembling the embryonic localization of heart formation.

Next, we aimed for testing the feasibility of chimeric gastruloids for the assessment of cell-autonomous vs. cell non-autonomous functions of *Brachyury* during posterior elongation, as the shortening of the posterior body axis is the most prominent phenotype of *Brachyury*-mutant embryos (Fig. 3A)(Wymeersch et al., 2021). Gastruloids entirely generated from mT-labelled *Bra*$^{-/-}$ mESCs present with a phenotype of impaired elongation, similar to shortened tailbuds observed in *Brachyury*-mutant embryos (Fig. 3B, C) (Inman and Downs, 2006). Increasing the proportional contribution of WT cells (mG) to the gastruloid by intermixing WT with *Bra*$^{-/-}$ mESCs during the initial aggregation of 300 ESCs leads to the gradual extension and increase in overall mass of the posterior portion of the mixed gastruloids (Fig. 3C). Interestingly, in the tail bud region of chimeric gastruloids with a contribution of *Bra*$^{-/-}$ cells of 90%, *Brachyury* expression is also absent in WT cells when compared to chimeric gastruloids where *Bra*$^{-/-}$ cell contribution is only 50%, and Brachyury expression is robustly induced in the posterior pole (Fig. 3D). The cell non-autonomous contribution of *Bra*$^{-/-}$ cells to disturbances of axis-extension is most likely explained by the previously described feed-forward regulation of *Wnt3a* and *Brachyury* in the tail-bud region (Arnold et al., 2000; Dunty et al., 2008; Martin and Kimelman, 2008; Turner et al., 2014; Yamaguchi et al., 1999).

Finally, in addition to the gross, tissue-wide phenotype of *Brachyury*-deficiency in gastruloids with a high ratio of *Bra*$^{-/-}$ cells, we analyzed the cell-autonomous effects of *Brachyury*-deficiency in conditions of low contribution of mutant cells (Fig. 4). We generated chimeric gastruloids by mixing cells in a 90:10 ration of WT and *Bra*$^{-/-}$ ESCs, respectively. In resulting gastruloids *Bra*$^{-/-}$ cells show a specific tissue distribution, so that they are predominantly found along the midline in the interior of the gastruloids, and in the posterior pole (Fig. 4A). To determine tissue identity of these regions we used immunofluorescence (IF) staining against FOXA2 and CDH1 (E-Cadherin), labelling DE (Viotti et al., 2014) and SOX2, labelling neuroectoderm (NE) cells (Wood and Episkopou, 1999), and combined IF-staining with the fluorescent labels of WT (mG) and *Bra*$^{-/-}$ cells (mT) (Fig. 4B, C). FOXA2 and CDH1 stainings indicate that *Bra*$^{-/-}$

cells are biased towards DE and are favored to form the gut tube-like structure in the midline. This finding demonstrates not only that *Brachyury* is dispensable for DE lineage specification from pluripotent cells, but suggests that *Brachyury* actually counteracts DE specification programs and thus may not represent a suitable marker for early DE-forming cells as previously suggested (Kubo et al., 2004). Staining against SOX2 shows that the *Bra*$^{-/-}$ cells that are present in the posterior pole of chimeric gastruloids mostly acquire NE fate, in accordance with previous findings about NE-repressive functions of *Brachyury* (Koch et al., 2017; Tosic et al., 2019).

In conclusion, this study illustrates a novel experimental approach by combining functional genetics in ESCs with 3D-gastruloids to form different types of chimeric gastruloids, that allow to experimentally address various aspects of development. Inducible expression of the Tbx transcription factor *Eomes* demonstrates how limitations of 3D gastruloids can be overcome by genetically providing regulatory cues that are missing or underrepresented in CHIR-only treated gastruloids, namely the induced formation of anterior mesoderm derivatives such as heart tissue. We additionally show how chimeric gastruloids can be employed to analyze cell-autonomous and cell non-autonomous gene-functions by varying the contribution of gene-mutant cells to chimeric gastruloids. Using a low ratio of only 10% of *Brachyury*-deficient cells we find that *Bra*$^{-/-}$ cells cell-autonomously are biased towards the DE, a cell lineage that strictly depends on *Eomes* functions (Arnold et al., 2008; Teo et al., 2011). Since *Brachyury* and *Eomes* are co-expressed in cells of the early primitive streak in early gastrulating embryos (Probst et al., 2021), this poses the interesting question about the regulatory interactions between these two related Tbx factors.

While in this study we used functional genetics of ESCs harbouring loss- and gain-of-gene function alleles, ESCs with other genetic modifications could also be applied in chimeric gastruloids, for example reporter-containing cells for signalling pathway (e.g. Wnt-signalling), cellular processes (e.g. cell migration and actin-dynamics), or protein-localization. Additionally, while in this study chimeric gastruloids contained only two different cell types, more cells of different genotype could be combined. This might be desirable, e.g. to observe morphogenetic processes by different reporter cell lines.

In summary, chimeric gastruloids represent powerful experimental tools for studies of gastrulation stage embryogenesis. In addition to the increased experimental accessibility, observability and scalability, chimeric gastruloids also allow to generate

complex genetic settings that are normally only difficult to achieve by genetics in embryos.

Materials and Methods

Cell lines

A2lox mouse ESCs (Iacovino et al., 2014) were cultured in Dulbecco's modified Eagle's medium (DMEM) containing 15 % fetal bovine serum (FBS, Gibco), 2 mM L-glutamine, 1X non-essential amino acids (NEAA), 1 mM sodium-pyruvate, 1X penicillin/streptomycin (all from Gibco), 100 µM β-mercaptoethanol (Sigma), Leukemia inhibitory factor (ESGRO LIF, Merck Millipore, 1000 U/ml), and 2i: CHIR99021 (Axon Medchem, 3 µM) and PD0325901 (Axon Medchem, 1 µM) on 0.1% gelatine-coated dishes. The medium was changed daily and ESCs were passaged every other day. The generation of *Bra*$^{-/-}$ ESCs and of A2lox ESCs harbouring dox- inducible expression cassette for *Eomes*.GFP were described previously (Tosic et al., 2019). A2lox cells with membrane-tagged fluorescent labels (membrane-Tomato, mT, and membrane-GFP, mG) were generated by targeted integration of a mT/mG targeting vector (Muzumdar et al., 2007), Addgene plasmid #17787) into the Rosa26 locus. 1x10^{6} A2lox ESCs (WT and *Bra*$^{-/-}$) were transfected with 2.5 µg of linearized vector using the Nucleofector ESC kit (Lonza) and G418 selected (350 µg/ml) on a monolayer of MitoC (Sigma)-mitotically inactivated STO feeder cells. mT-expressing ESC clones were picked on day 9 of selection. To convert the expression of the membrane-Tomato (mT) to membrane-GFP (mG) in WT A2lox ESCs, cells were treated for 24 h with 5 µg/ml Doxycyclin (Sigma, D9891) for induced expression of the Cre-recombinase from the Dox-inducible locus of A2lox WT cells to excise the loxP-flanked mT expression cassette and bring the mG expression cassette under the transcriptional control of the Rosa26 gene locus. After Cre-excision mG-expressing WT A2lox ESCs underwent one round of clonal selection by minimal dilution of 500 cells onto a 10 cm cell culture dish.

Generation of chimeric gastruloids

Gastruloids were generated using published protocols (van den Brink et al., 2020) with some modifications as outlined below. Gastruloid formation was performed in ESGRO Complete Basal Medium (Merck Millipore) in the absence of Matrigel. To generate chimeric gastruloids using different ESCs by merging of preformed aggregates 150 cells of each ESC line were aggregated in 40 µl of ESGRO basal medium in 96-well

format (Greiner ultra-low attachment plates, No. 650970) for 24 h before merging by combining two aggregates into the same well. At 48 h following first aggregate formation, fused gastruloids were induced by administration of 3 µM CHIR and if indicated with doxycycline (1 µg/µl, Sigma) for 24 h. In the course of gastruloid culture, the medium was changed daily at 72, 96, 120 and 144 h. For the generation of gastruloids by mixing of different ESC lines, aggregates were formed from a total of 300 ESCs at various rations between the two ESC lines, and further gastruloid formation followed by previously used protocols (van den Brink et al., 2020).

Whole mount *in situ* hybridization

Whole-mount in situ hybridization was performed according to standard protocols using previously published probes for *Mlc2a* and *Nkx2.5* (Costello et al., 2011). In brief, gastruloids were fixed in 4% PFA / PBS o/n at 4°C, dehydrated and stored in methanol at -20°C. After rehydration gastrulation were bleached in 6 % H_2O_2 for 5 min, digested by 1.6 µg / ml Proteinase K in PBT for 2 min, and postfixed in 4% PFA / 0,2% glutaraldehyde for 20 min before prehybridization for 2 h and hybridization o/n according to standard protocols. DIG-labelled RNA probe was detected using anti-Digoxigenin-AP Fab fragments (Roche) in 1% sheep serum, 2% BBR in MAB (0.1 M Maleic acid, 0.3 M NaCl, NaOH, 1% Tween-20 in H_2O, pH 7.5) and incubation at 4°C o/n. Antibody was washed out by extensive washes in MAB (>24 h, RT), and color reaction performed in BM purple staining solution (Roche) for 2-6 h at RT.

Immunofluorescence staining

Gastruloids were fixed in 4% PFA /PBS for 1 h at 4°C, permeabilized (0.3% Triton X-100/ PBT, 30 min) and blocked in 1% BSA / PBT for 1h at RT. Primary antibody incubation was performed at 4°C o/n in 1% BSA / PBT, gastruloids washed 4x in PBT before secondary fluorescence-conjugated antibody incubation for 3 h followed by DAPI staining for 30 min at RT. Primary antibodies used were BRACHYURY (R&D Systems; AF2085), FOXA2 (Cell Signaling; 8186S), E-Cadherin (BD Transduction Laboratories; 610182) and SOX2 (R&D Systems; AF2018) at suggested dilutions. Secondary anti-goat, anti-rabbit and anti-mouse Alexa Fluor 647-conjugated antibodies (Thermo Fisher) were used at 1:1000 dilutions.

Imaging

Images were acquired on a Leica DMi8 Thunder Imager System or a Leica M165FC Stereo microscope. Images were processed in the Leica LASX software and Affinity Photo. During time lapse imaging gastruloids were maintained under constant conditions at 37°C, 5% CO_2.

Acknowledgements

We thank T. Bass for excellent technical assistance and Michael Kyba for the A2lox ESC line.

Funding

This work was supported by the German Research Foundation (DFG) through the Heisenberg Program (AR 732/3-1), project grant (AR 732/2-1,) project B07 of SFB 1140 (project ID 246781735), project A03 of SFB 850 (project ID 89986987), project P7 of SFB 1453 (project ID 431984000), and Germany's Excellence Strategy (CIBSS – EXC-2189 – Project ID 390939984) to S.J.A., and by the MOTI-VATE program of the Freiburg Medical Faculty supported by the Else-Kröner-Fresenius-Stiftung to A.C.

Competing interests

The authors declare no competing interests.

Author contributions

A.E.W., K.M.S., A.C., C.M.S. generated different ESC lines and performed experiments. A.E.W, S.P. and S.J.A. planned and analyzed experiments. A.E.W. and S.J.A. prepared figures, wrote and edited the manuscript with input from all authors. S.J.A. conceived the study.

References

Amadei, G., Lau, K. Y. C., De Jonghe, J., Gantner, C. W., Sozen, B., Chan, C., Zhu, M., Kyprianou, C., Hollfelder, F. and Zernicka-Goetz, M. (2021). Inducible Stem-Cell-Derived Embryos Capture Mouse Morphogenetic Events In Vitro. *Dev Cell* **56**, 366-382 e369.

Arnold, S. J., Hofmann, U. K., Bikoff, E. K. and Robertson, E. J. (2008). Pivotal roles for eomesodermin during axis formation, epithelium-to-mesenchyme transition and endoderm specification in the mouse. *Development* **135**, 501-511.

Arnold, S. J. and Robertson, E. J. (2009). Making a commitment: cell lineage allocation and axis patterning in the early mouse embryo. *Nat Rev Mol Cell Biol* **10**, 91-103.

Arnold, S. J., Stappert, J., Bauer, A., Kispert, A., Herrmann, B. G. and Kemler, R. (2000). Brachyury is a target gene of the Wnt/beta-catenin signaling pathway. *Mech Dev* **91**, 249-258.

Beccari, L., Moris, N., Girgin, M., Turner, D. A., Baillie-Johnson, P., Cossy, A. C., Lutolf, M. P., Duboule, D. and Arias, A. M. (2018). Multi-axial self-organization properties of mouse embryonic stem cells into gastruloids. *Nature* **562**, 272-276.

Costello, I., Pimeisl, I. M., Drager, S., Bikoff, E. K., Robertson, E. J. and Arnold, S. J. (2011). The T-box transcription factor Eomesodermin acts upstream of Mesp1 to specify cardiac mesoderm during mouse gastrulation. *Nat Cell Biol* **13**, 1084-1091.

Dunty, W. C., Jr., Biris, K. K., Chalamalasetty, R. B., Taketo, M. M., Lewandoski, M. and Yamaguchi, T. P. (2008). Wnt3a/beta-catenin signaling controls posterior body development by coordinating mesoderm formation and segmentation. *Development* **135**, 85-94.

Harrison, S. E., Sozen, B., Christodoulou, N., Kyprianou, C. and Zernicka-Goetz, M. (2017). Assembly of embryonic and extraembryonic stem cells to mimic embryogenesis in vitro. *Science* **356**.

Harrison, S. E., Sozen, B. and Zernicka-Goetz, M. (2018). In vitro generation of mouse polarized embryo-like structures from embryonic and trophoblast stem cells. *Nat Protoc* **13**, 1586-1602.

Iacovino, M., Roth, M. E. and Kyba, M. (2014). Rapid genetic modification of mouse embryonic stem cells by Inducible Cassette Exchange recombination. *Methods Mol Biol* **1101**, 339-351.

Inman, K. E. and Downs, K. M. (2006). Brachyury is required for elongation and vasculogenesis in the murine allantois. *Development* **133**, 2947-2959.

Kagawa, H., Javali, A., Khoei, H. H., Sommer, T. M., Sestini, G., Novatchkova, M., Scholte Op Reimer, Y., Castel, G., Bruneau, A., Maenhoudt, N., et al. (2022). Human blastoids model blastocyst development and implantation. *Nature* **601**, 600-605.

Koch, F., Scholze, M., Wittler, L., Schifferl, D., Sudheer, S., Grote, P., Timmermann, B., Macura, K. and Herrmann, B. G. (2017). Antagonistic Activities of Sox2 and Brachyury Control the Fate Choice of Neuro-Mesodermal Progenitors. *Dev Cell* **42**, 514-526 e517.

Kubo, A., Shinozaki, K., Shannon, J. M., Kouskoff, V., Kennedy, M., Woo, S., Fehling, H. J. and Keller, G. (2004). Development of definitive endoderm from embryonic stem cells in culture. *Development* **131**, 1651-1662.

Li, R., Zhong, C., Yu, Y., Liu, H., Sakurai, M., Yu, L., Min, Z., Shi, L., Wei, Y., Takahashi, Y., et al. (2019). Generation of Blastocyst-like Structures from Mouse Embryonic and Adult Cell Cultures. *Cell* **179**, 687-702 e618.

Martin, B. L. and Kimelman, D. (2008). Regulation of canonical Wnt signaling by Brachyury is essential for posterior mesoderm formation. *Dev Cell* **15**, 121-133.

Moris, N., Anlas, K., van den Brink, S. C., Alemany, A., Schroder, J., Ghimire, S., Balayo, T., van Oudenaarden, A. and Martinez Arias, A. (2020). An in vitro model of early anteroposterior organization during human development. *Nature* **582**, 410-415.

Muzumdar, M. D., Tasic, B., Miyamichi, K., Li, L. and Luo, L. (2007). A global double-fluorescent Cre reporter mouse. *Genesis* **45**, 593-605.

Probst, S., Sagar, Tosic, J., Schwan, C., Grun, D. and Arnold, S. J. (2021). Spatiotemporal sequence of mesoderm and endoderm lineage segregation during mouse gastrulation. *Development* **148**.

Rivera-Perez, J. A. and Magnuson, T. (2005). Primitive streak formation in mice is preceded by localized activation of Brachyury and Wnt3. *Dev Biol* **288**, 363-371.

Rossi, G., Broguiere, N., Miyamoto, M., Boni, A., Guiet, R., Girgin, M., Kelly, R. G., Kwon, C. and Lutolf, M. P. (2021). Capturing Cardiogenesis in Gastruloids. *Cell Stem Cell* **28**, 230-240 e236.

Teo, A. K., Arnold, S. J., Trotter, M. W., Brown, S., Ang, L. T., Chng, Z., Robertson, E. J., Dunn, N. R. and Vallier, L. (2011). Pluripotency factors regulate definitive endoderm specification through eomesodermin. *Genes Dev* **25**, 238-250.

Tosic, J., Kim, G. J., Pavlovic, M., Schroder, C. M., Mersiowsky, S. L., Barg, M., Hofherr, A., Probst, S., Kottgen, M., Hein, L., et al. (2019). Eomes and Brachyury control pluripotency exit and germ-layer segregation by changing the chromatin state. *Nat Cell Biol* **21**, 1518-1531.

Turner, D. A., Girgin, M., Alonso-Crisostomo, L., Trivedi, V., Baillie-Johnson, P., Glodowski, C. R., Hayward, P. C., Collignon, J., Gustavsen, C., Serup, P., et al. (2017). Anteroposterior polarity and elongation in the absence of extra-embryonic tissues and of spatially localised signalling in gastruloids: mammalian embryonic organoids. *Development* **144**, 3894-3906.

Turner, D. A., Rue, P., Mackenzie, J. P., Davies, E. and Martinez Arias, A. (2014). Brachyury cooperates with Wnt/beta-catenin signalling to elicit primitive-streak-like behaviour in differentiating mouse embryonic stem cells. *BMC Biol* **12**, 63.

van den Brink, S. C., Alemany, A., van Batenburg, V., Moris, N., Blotenburg, M., Vivie, J., Baillie-Johnson, P., Nichols, J., Sonnen, K. F., Martinez Arias, A., et al. (2020). Single-cell and spatial transcriptomics reveal somitogenesis in gastruloids. *Nature* **582**, 405-409.

van den Brink, S. C., Baillie-Johnson, P., Balayo, T., Hadjantonakis, A. K., Nowotschin, S., Turner, D. A. and Martinez Arias, A. (2014). Symmetry breaking, germ layer specification and axial organisation in aggregates of mouse embryonic stem cells. *Development* **141**, 4231-4242.

van den Brink, S. C. and van Oudenaarden, A. (2021). 3D gastruloids: a novel frontier in stem cell-based in vitro modeling of mammalian gastrulation. *Trends Cell Biol* **31**, 747-759.

Veenvliet, J. V., Bolondi, A., Kretzmer, H., Haut, L., Scholze-Wittler, M., Schifferl, D., Koch, F., Guignard, L., Kumar, A. S., Pustet, M., et al. (2020). Mouse embryonic stem cells self-organize into trunk-like structures with neural tube and somites. *Science* **370**.

Veenvliet, J. V., Lenne, P. F., Turner, D. A., Nachman, I. and Trivedi, V. (2021). Sculpting with stem cells: how models of embryo development take shape. *Development* **148**.

Viotti, M., Nowotschin, S. and Hadjantonakis, A. K. (2014). SOX17 links gut endoderm morphogenesis and germ layer segregation. *Nat Cell Biol* **16**, 1146-1156.

Wood, H. B. and Episkopou, V. (1999). Comparative expression of the mouse Sox1, Sox2 and Sox3 genes from pre-gastrulation to early somite stages. *Mech Dev* **86**, 197-201.

Wymeersch, F. J., Wilson, V. and Tsakiridis, A. (2021). Understanding axial progenitor biology in vivo and in vitro. *Development* **148**.

Xu, P. F., Borges, R. M., Fillatre, J., de Oliveira-Melo, M., Cheng, T., Thisse, B. and Thisse, C. (2021). Construction of a mammalian embryo model from stem cells organized by a morphogen signalling centre. *Nat Commun* **12**, 3277.

Yamaguchi, T. P., Takada, S., Yoshikawa, Y., Wu, N. and McMahon, A. P. (1999). T (Brachyury) is a direct target of Wnt3a during paraxial mesoderm specification. *Genes Dev* **13**, 3185-3190.

Yu, L., Wei, Y., Duan, J., Schmitz, D. A., Sakurai, M., Wang, L., Wang, K., Zhao, S., Hon, G. C. and Wu, J. (2021). Blastocyst-like structures generated from human pluripotent stem cells. *Nature* **591**, 620-626.

FIGURE LEGENDS

Fig. 1. Experimental approaches for the generation of chimeric gastruloids

(A) Schematic of two alternative experimental approaches to generate chimeric gastruloids from fluorescently labelled embryonic stem cells (ESCs). Wildtype (WT) ESCs are marked by membrane-GFP (mG) and combined with membrane-Tomato (mT) labelled, genetically modified ESCs. The genetic modifications of ESCs comprise homozygous gene deletions (GeneX) or inducible gene-expression by the targeting of cDNAs into a fully controllable pre-engineered locus containing a Tetracycline

responsive element (TRE) for dox-dependent induction of gene expression (GeneY). Chimeric gastruloids are generated by either mixing of ESCs at the beginning of gastruloid culture, or by merging preformed ESCs aggregates proceeding the induction of gastruloids by CHIR. Chimeric gastruloids can be used as versatile novel model system for various types of studies and embryonic research questions as indicated exemplary.

(B) Schematic of the protocol to form chimeric gastruloids indicating timepoints for either mixing of cells, or merging of aggregates to create chimeric gastruloids.

(C) Membrane-GFP (mG) labelling of WT ESCs and membrane-Tomato (mT) labelling for genetically modified ESCs allows for distinguishing different cell types in chimeric gastruloids. Scale bars 10 µm.

(D) Timelapse-imaging of the merging process of pre-formed ESC aggregates at indicated time points. 150 mG and mT ESCs were aggregated for 24 h before merging them by placing them together in 96-well plates. After 1 hr two aggregates spontaneously aggregated and formed stable contacts. Scale bars 100 µm. Also see **Supplementary Movie 1** for a 12 h time-lapse movie.

(E) Examples of mixed ESC aggregates at 24 h after aggregation of 300 ESCs by mixing mG WT ESCs and mT Bra$^{-/-}$ ESCs at indicated rations. Scale bars 100µm.

Fig. 2. Instructive functions of *Eomes* for cardiac lineage specification in merged chimeric gastruloids.

(A) Schematic illustrating the generation and culture of chimeric gastruloids by merging preformed aggregated of mG-labelled WT ESCs and mT-labelled ESCs harbouring *EomesGFP* in the Doxycycline (Dox)-inducible gene locus (TRE.*EomesGFP, short* TRE.*Eo*).

(B) Fluorescent microscopy of TRE.*EomesGFP* ESCs showing nuclear staining of doxycycline-induced (+DOX) EOMES.GFP after 24 h of administration that is absent in -DOX conditions. Scale bars 10 µm.

(C) Brightfield (left) and fluorescent (right) images of a chimeric gastruloid following induced *Eomes* expression showing the region of beating cardiomyocytes within the gastruloid that is mostly derived of mT-labelled TRE.*EomesGFP* cells. The dashed line indicates the domain of beating cells. Scale bars 100 µm. See also **Supplementary Movie 2** for the corresponding time-lapse movie.

(D) Statistics comparing the percentage of beating gastruloids at 168 h following forced *Eomes* expression +DOX (33,3% ± 3,01) and uninduced controls -DOX (1,5% ± 2,31) in n=3 independent experiments. Error bar indicates SEM.
(E) Fluorescent microscopy (left) and whole-mount *in situ* hybridization (right) of the same chimeric gastruloids following induced *Eomes*-expression (+DOX) shows the instructive functions of forced *Eomes*-expression in TRE.*EomesGFP* cells for the induction of cardiac progenitors, indicated by expression of *Mlc2a* and *Nkx2.5.* Scale bars 100 µm.

Fig. 3. Analyses of *Brachyury* functions during axis-elongation in chimeric gastruloids generated by cell mixing.
(A) Schematic illustrating the generation of chimeric gastruloids by mixing of mG-labelled WT ESCs and mT-labelled Brachyury-deficient (*Bra*$^{-/-}$) ESCs.
(B) Immunofluorescence stainings for BRACHYURY in gastruloids at 120 h generated from either WT or *Bra*$^{-/-}$ cells showing the presence of BRACHYURY in the posterior pole of the WT, and absence in *Bra*$^{-/-}$ derived gastruloids that fail to elongate.
(C) Chimeric gastruloids at 120 h generated by mixing of *Bra*$^{-/-}$ (mT) and WT (mG) ESCs at indicated rations of cell numbers. Gastruloids with a contribution of *Bra*$^{-/-}$ cells above 80 % show reduced axial elongation. Gastruloids entirely generated from *Bra*$^{-/-}$ cells fail to extend beyond an oval shape. At WT (mG) cell contribution > 50 % axial elongation is similar to WT gastruloids but occasionally shows a thinning of the posterior portion. Across all experiments *Bra*$^{-/-}$ (mT) cells preferentially contribute to the posterior portion of mixed gastruloids. In all images anterior is to the top and posterior to the bottom of the picture.
(D) Immunofluorescence staining for BRACHYUY in gastruloids generated by cell mixing of *Bra*$^{-/-}$ and WT in rations of 90:10 and 50:50 show the absence of BRACHYUY from WT cells (arrows) at the posterior pole in gastruloids with a high contribution of *Bra*$^{-/-}$ cells (90% contribution) by cell non-autonomous mechanisms. Scale bars 100 µm in B-D.

Fig. 4. Cell-autonomous effects of Brachyury-deficiency on cell lineage specification and tissue sorting in chimeric gastruloids with low contribution of *Bra*$^{-/-}$ cells

(A) Three independent replicates of chimeric gastruloids at 120 h generated by mixing of 10% *Bra*$^{-/-}$ (mT) and 90 % WT (mG) ESCs at the start of the experiment show an enrichment of *Bra*$^{-/-}$ cells along the midline of the gastruloids and the posterior pole. The three replicates indicate the spectrum of distribution of *Bra*$^{-/-}$ cells found in chimeric gastruloids.
(B) Immunofluorescence stainings for the definitive endoderm marker FOXA2 and the epithelial marker CDH1 (E-Cadherin) show the predominant contribution of *Bra*$^{-/-}$ cells to endoderm-like cells forming the primary gut tube (arrow) of gastruloids, and some enrichment of *Bra*$^{-/-}$ cells in the posterior region, reflecting the tail bud region (boxed).
(C) *Bra*$^{-/-}$ cells that don't contribute to the epithelial primary gut tube of mixed gastruloids show nuclear SOX2-staining suggesting lineage commitment to neuroectoderm cell types. Scale bars 100 µm in A-C.

A

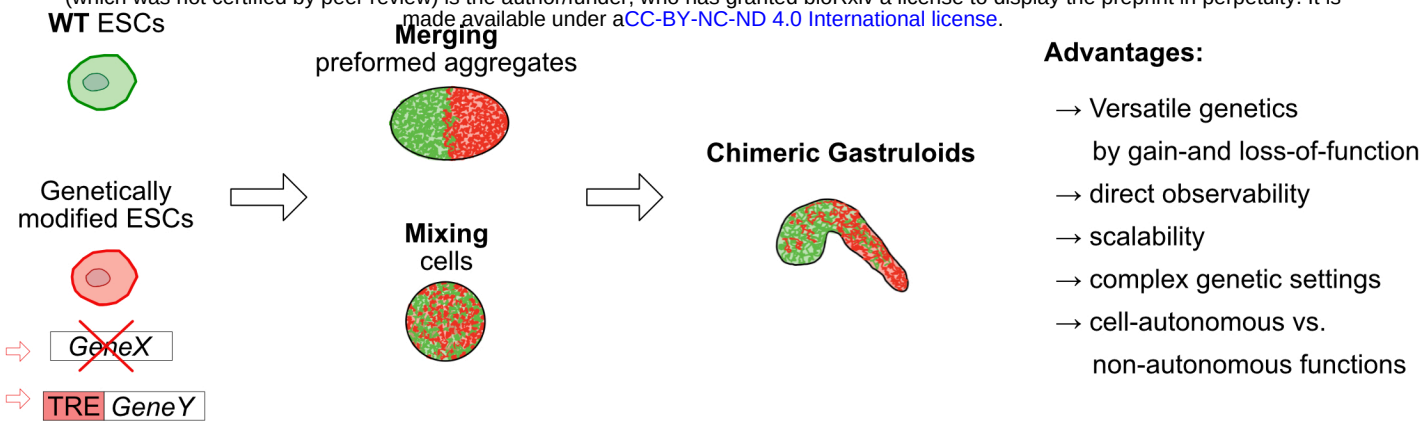

B

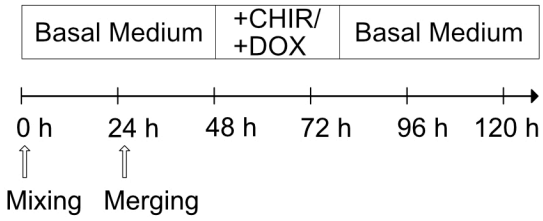

C

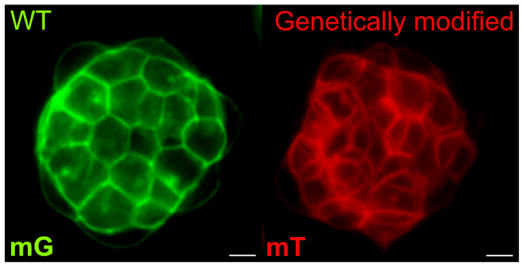

D

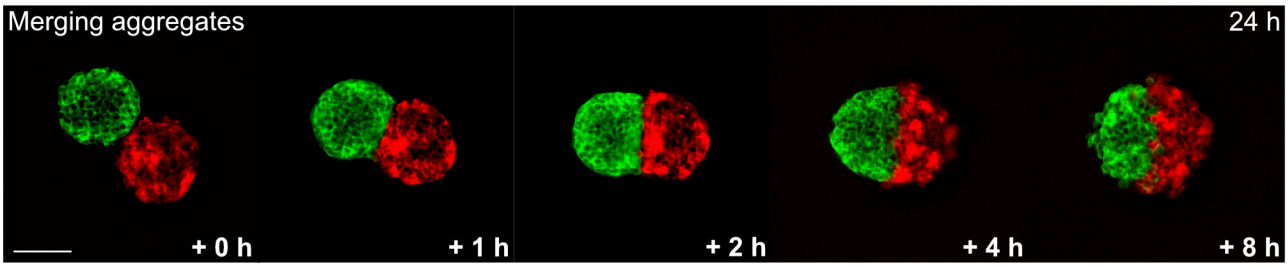

E

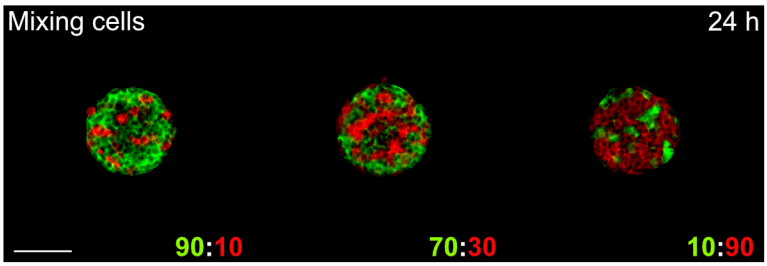

Fig. 1

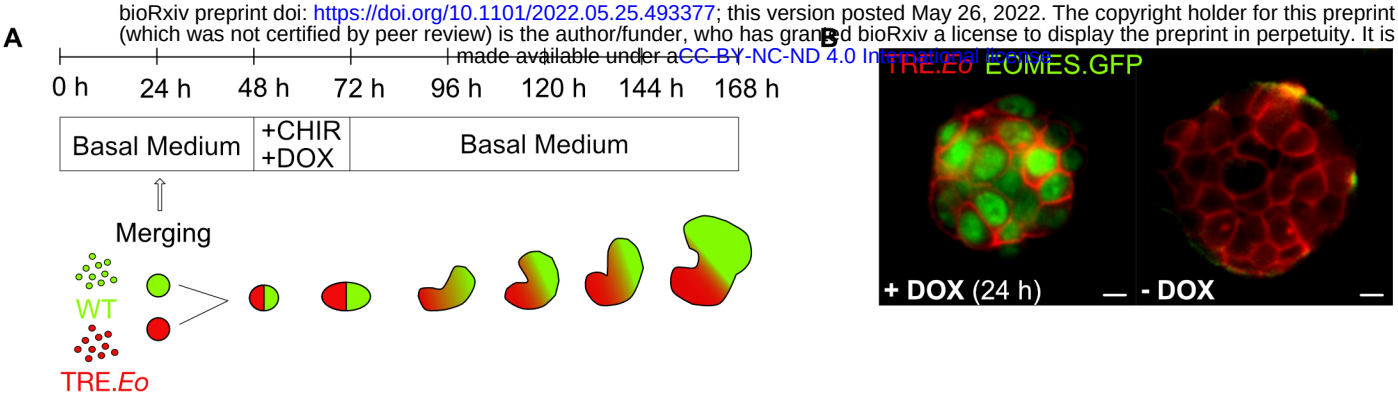

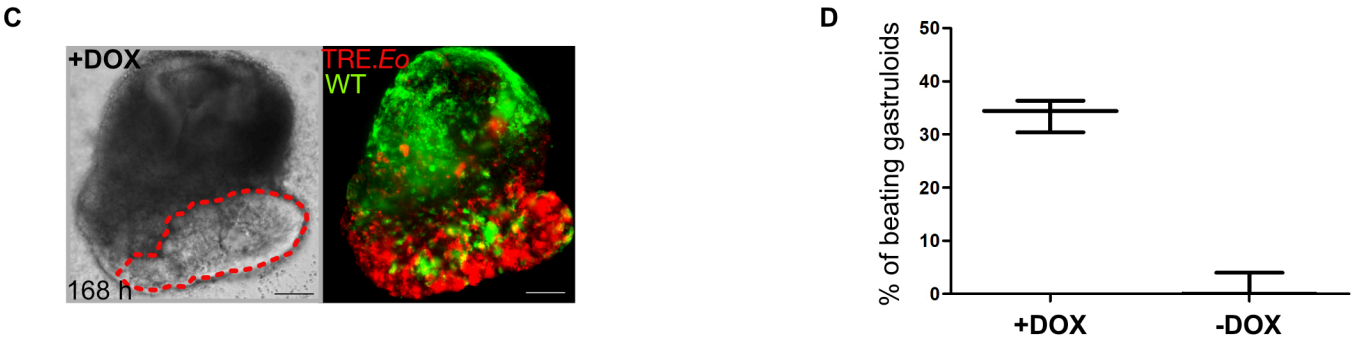

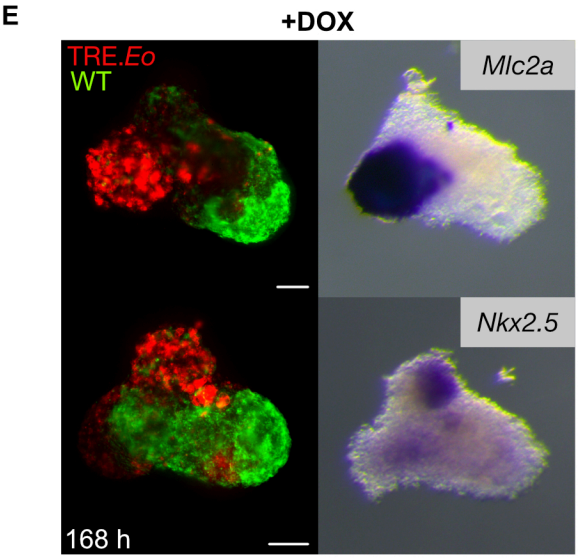

Fig. 2

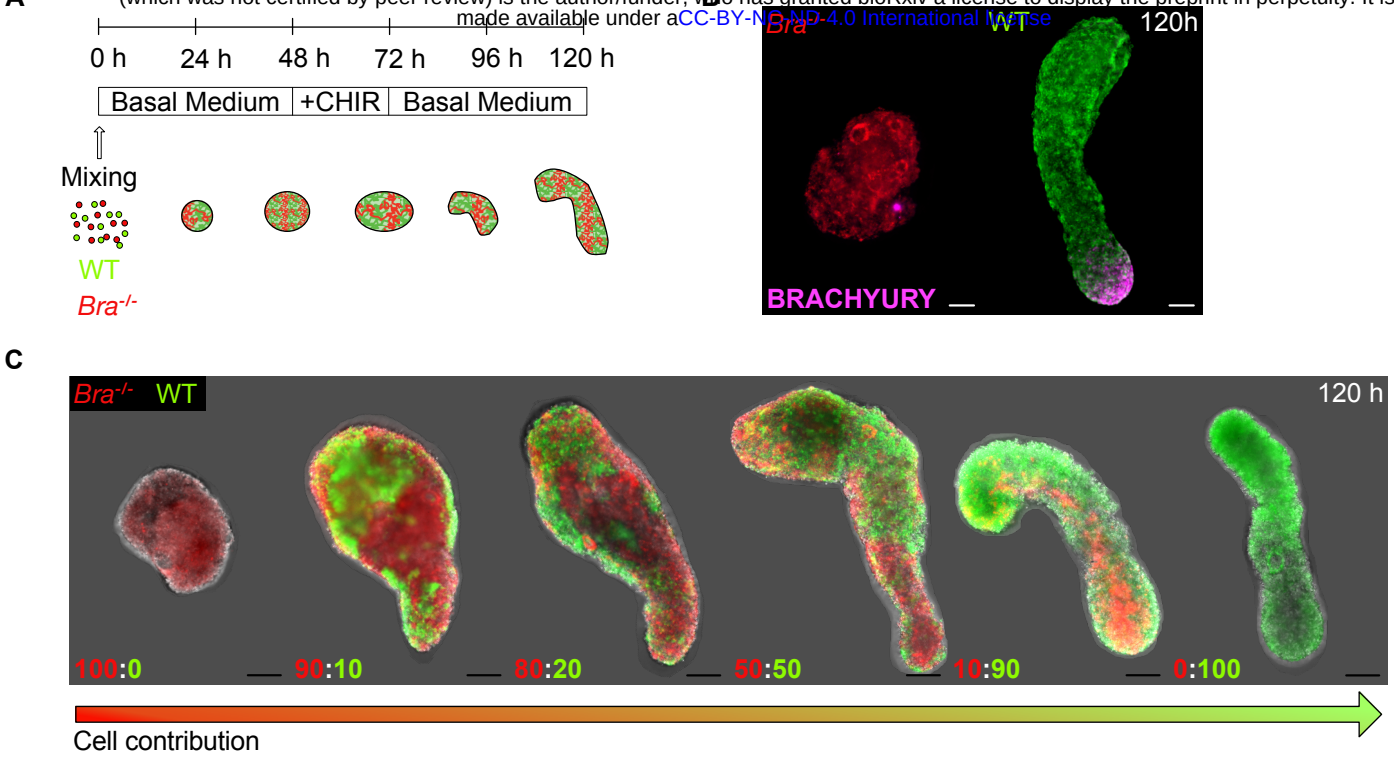

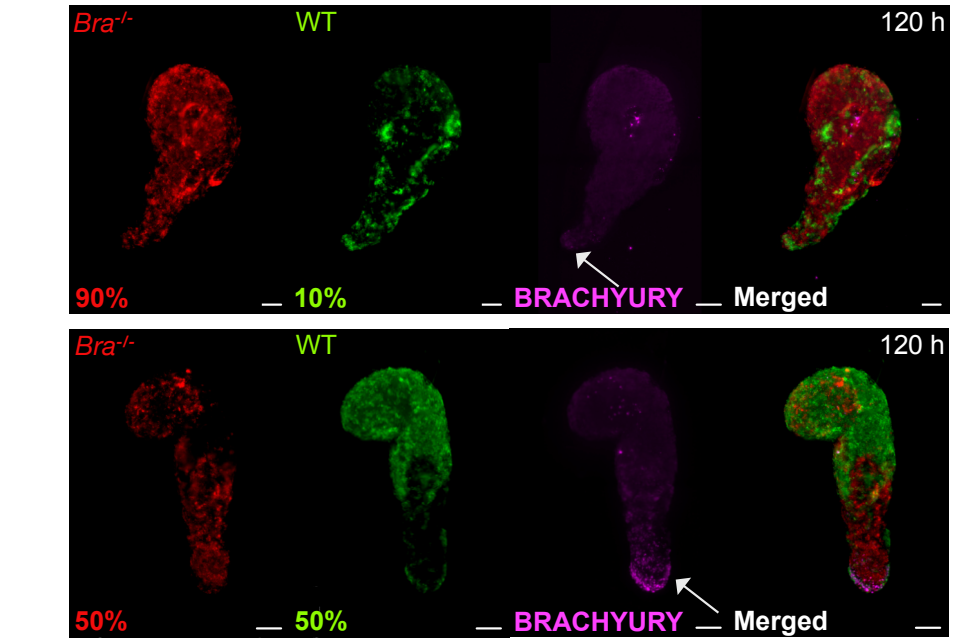

Fig. 3

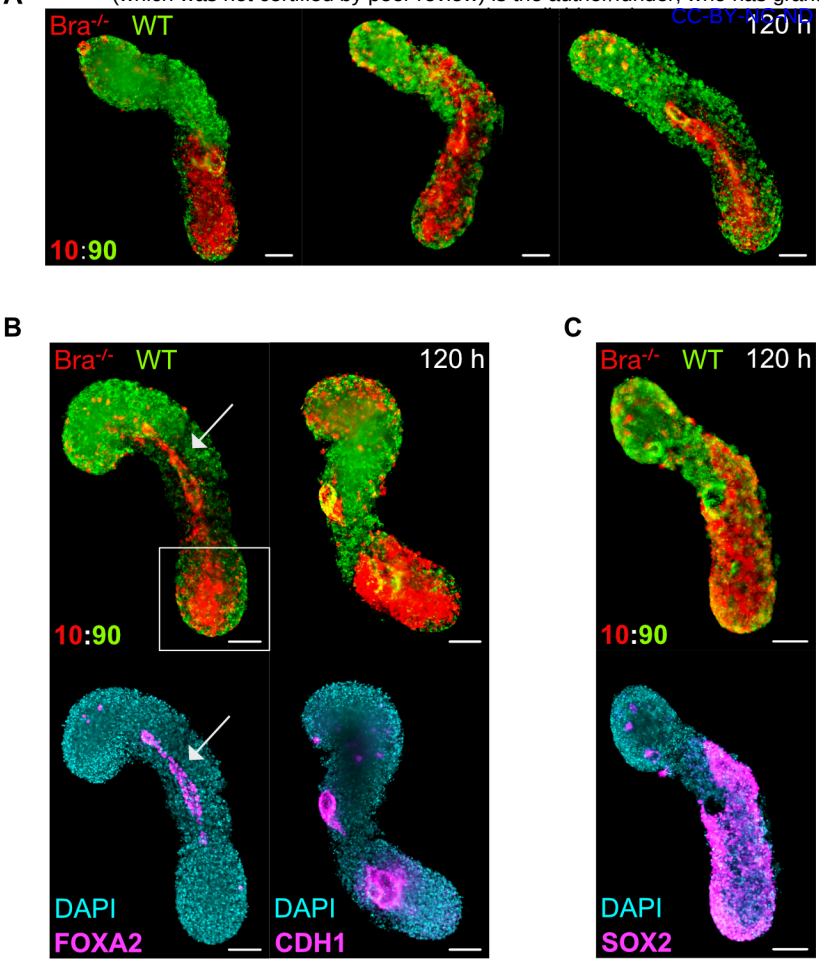

Fig. 4